Supplement of Geosci. Model Dev., 13, 6201–6213, 2020
https://doi.org/10.5194/gmd-13-6201-2020-supplement

Geoscientific Model Development
Open Access
EGU

Supplement of

Calibrating soybean parameters in JULES 5.0 from the US-Ne2/3 FLUXNET sites and the SoyFACE-O_3 experiment

Felix Leung et al.

Correspondence to: Felix Leung (felix.leung@cuhk.edu.hk)

Supplementary Material

We tuned the soybean physiology following a standard procedure as documented in Williams et al., (2017). Here we described the methods of tuning JULES against Mead observation without O_3 damage module turned on. The steps are described in Figure 1 and the detail of Step 1 to Step 5 are presented here.

1. Experimental set-up

1.1 Observations

We used plant physiology observations and meteorological data from FLUXNET, a global network of micrometeorological tower sites that use eddy covariance methods to measure the exchanges of carbon dioxide, water vapour, and energy between the biosphere and atmosphere. The Mead FLUXNET sites at the University of Nebraska-Lincoln Eastern Nebraska Research and Extension Center near Mead, Nebraska, USA are selected to tune the parameterization of the JULES-crop model for soybean. There are three FLUXNET sites at this location: US-Ne1 (irrigated maize), US-Ne2 (irrigated maize-soybean rotation) and US-Ne3 (rainfed maize-soybean rotation) (Suyker et al., 2004; Verma et al., 2005; Williams et al., 2017). Observations of maize at these sites have been used to calibrate the representation of irrigated maize in JULES-crop in Williams et al. (2017). Here, we use the same procedure to calibrate the representation of soybean based on the data from US-Ne2 and US-Ne3. Observations were available for biomass pools (green leaves, yellow leaves, stems, reproductive organs, and grains), leaf nitrogen, absorbed Photosynthetic Active Radiation (APAR), gross primary productivity (GPP), canopy height and defoliation-measured leaf area index (LAI), and meteorological variables. Most variables are used to tune the parameters required to simulate soybean in JULES-crop. The tuned parameters are summarized in Tables 1,2 and 3.

1.2 Step 1: Tune parameters required by all PFT tiles

In this section, we tune the parameters that are required by all vegetation tiles in the model. These govern the canopy structure, leaf photosynthesis and respiration.

The canopy parameter is tuned to fit the observed relation between Fraction of Absorbed Photosynthetically Active Radiation (FAPAR) and Leaf Area Index (LAI) is shown in Figure S1-1 , (top row), Using the default value of the canopy clumping factor $a = 1$ (i.e. a uniform canopy) leads to an overestimation of FAPAR at intermediate values of LAI (Figure S1-1, middle row). A lower structure factor of $a = 0.8$ compares better to the observations (bottom row, Figure S1-1). Figure S1-2 shows the value of the structure factor that would be needed to reproduce each FAPAR observation, given the observed LAI and diffuse radiation fraction.

Figure S1-3 shows the mean canopy leaf nitrogen to carbon mass ratio (left) and mean canopy leaf nitrogen per unit leaf area (right), while Figure S1-4 shows the top of canopy leaf nitrogen per unit leaf area assuming $k_{nl} = 0.2$. Figure S1-5 shows the relationship between hourly GPP and absorbed PAR for different diffuse radiation fractions in the observations (left) and the model (right), and was used to tune the quantum efficiency of photosynthesis and the maximum rate of carboxylation of Rubisco.

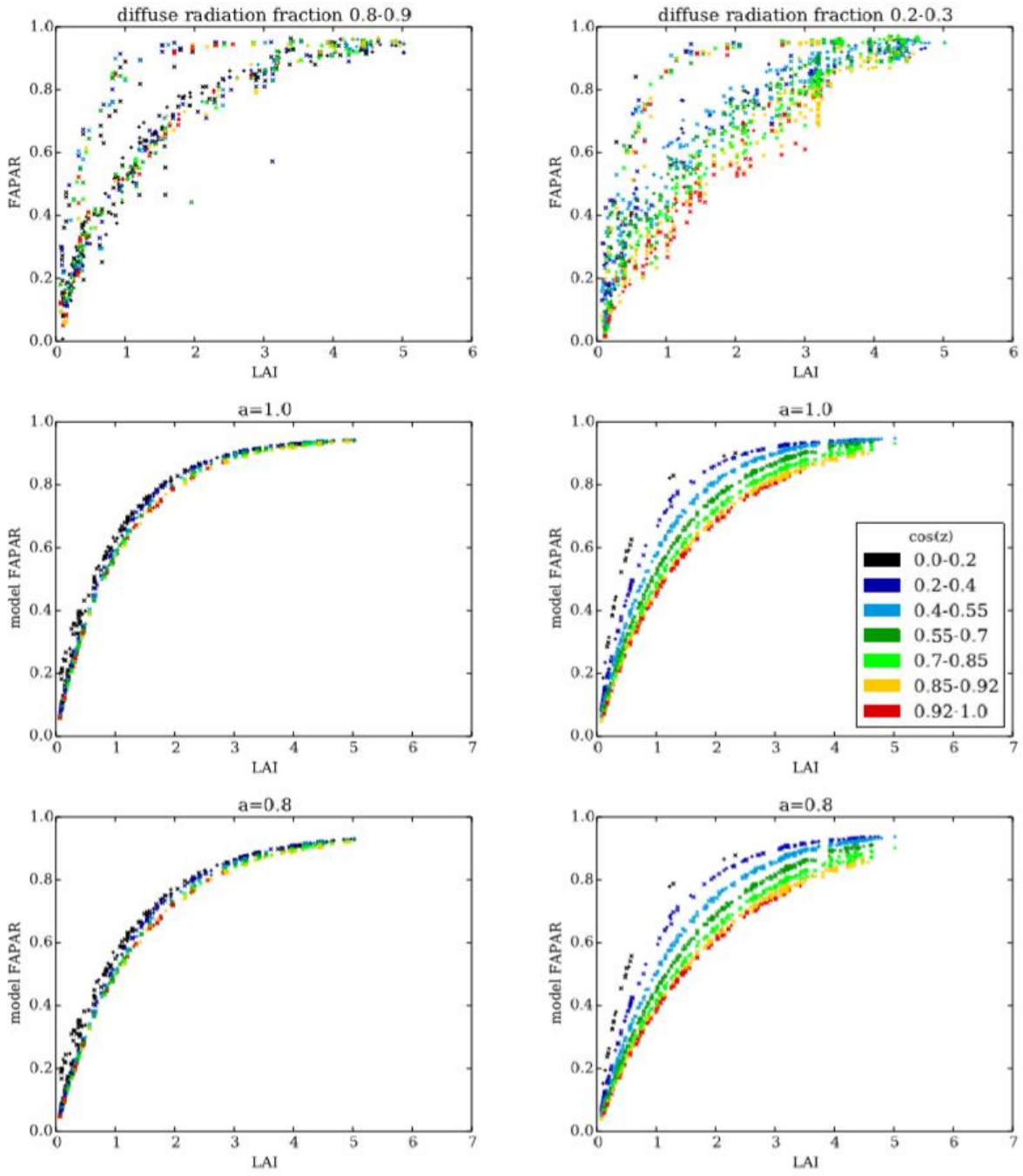

Figure S1-1. FAPAR against interpolated LAI observations. Top row uses FAPAR observations, middle and bottom rows use model FAPAR with $a = 1$ and $a = 0.8$ respectively, using observed LAI and diffuse radiation fractions. Vertical crosses (+) and diagonal crosses (x) show US-Ne2 and US-Ne3 respectively and all data are between DVI=0 and DVI=1.5. Colours show the cosine of the zenith angle.

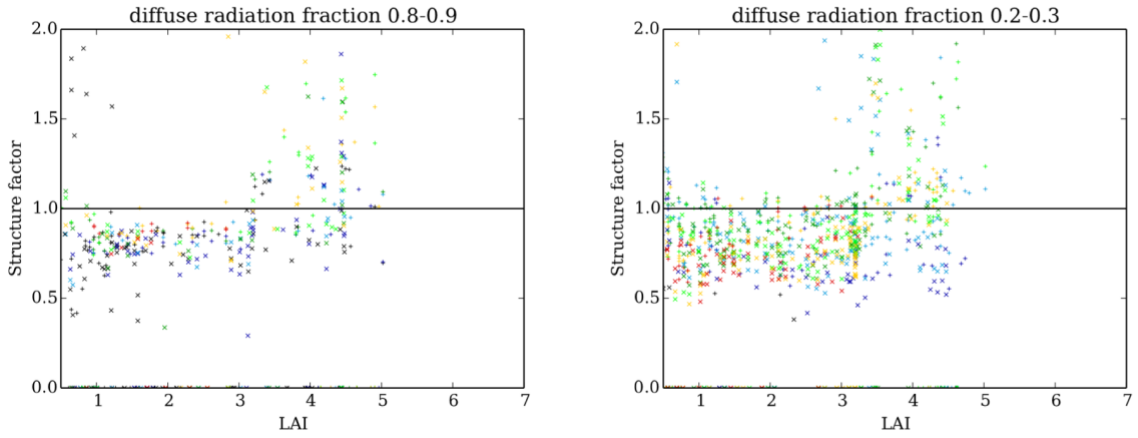

Figure S1-2. Derived value of the clumping factor *a* against LAI for each combination of FAPAR and observed diffuse radiation fraction. Vertical crosses (+) and diagonal crosses (x) use US-Ne2 and US-Ne3 LAI observations respectively and all data are between emergence (DVI=0) and flowering (DVI=1.5). Colours show the cosine for the zenith angle (for legend, see Figure S1-1). Solid black line indicates $a = 1$.

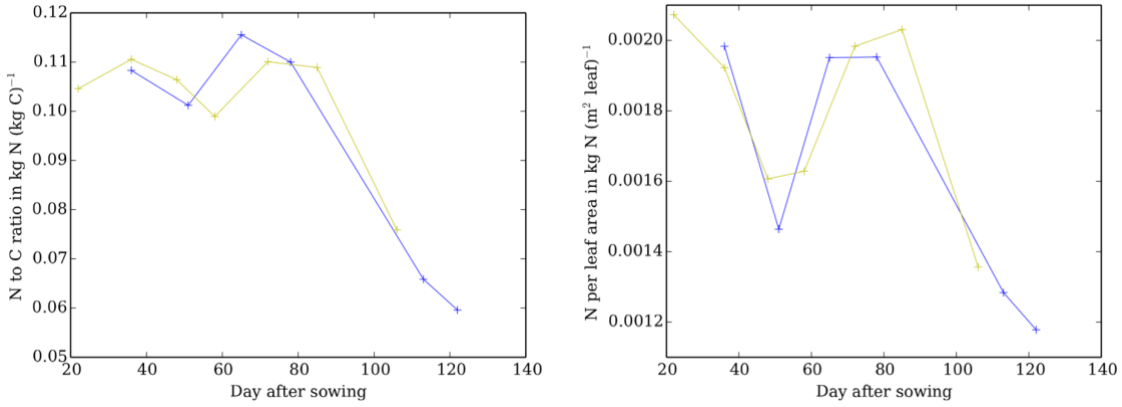

Figure S1-3. Observed ratio of nitrogen mass to carbon mass in leaves (left) and leaf nitrogen per leaf area (right) against day after sowing (canopy mean) at US-Ne2 (blue: 2002, yellow: 2004). $k_{nl} = 0$ i.e. leaf properties are assumed constant through the canopy.

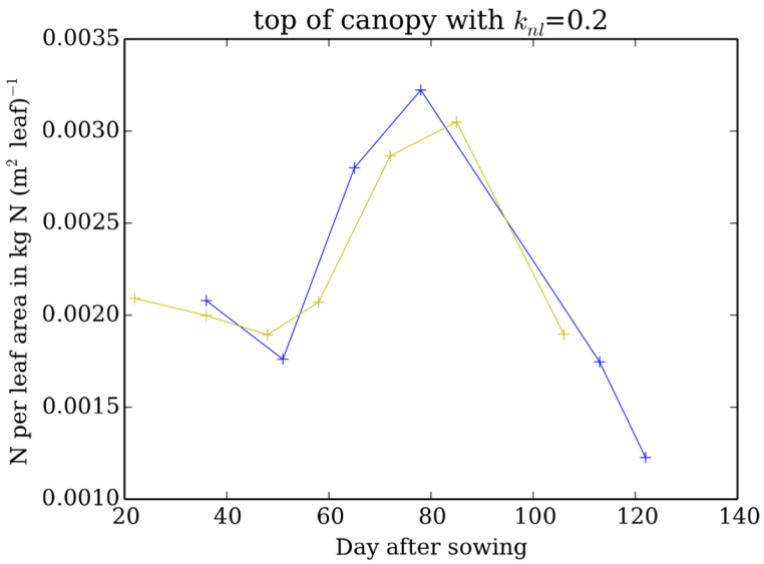

Figure S1-4. Observed leaf nitrogen per leaf area at top of canopy against day after sowing assuming a decay through the canopy with decay constant k_{nl} = 0.2 at US-Ne2 (blue: 2002, yellow: 2004)

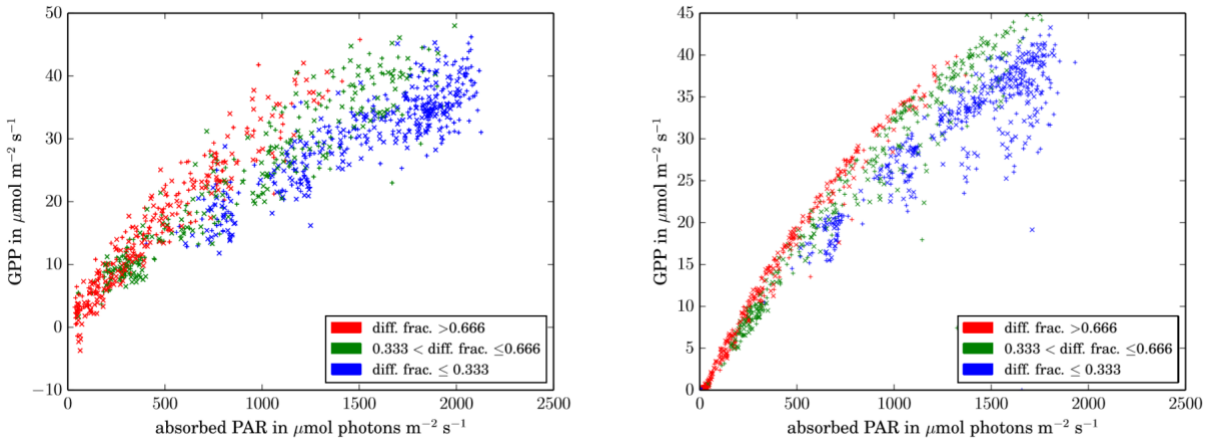

Figure S1-5. GPP (in μmol CO2(m^{2}ground)$^{-1}$s^{-1}) against incident PAR (in μmol photons (m^{2}ground)$^{-1}$s^{-1}) for the hourly FLUXNET data (left) and hourly output from the model runs (right). LAI is between 3.5 and 4.5 and all points have DVI less than 1.5. Vertical crosses (+) and diagonal crosses (x) indicate US-Ne2 and US-Ne3 respectively. Colour: diffuse radiation fraction. JULES runs have the crop model switched off, LAI and canopy height prescribed and the new input parameters in Table 3, Table 2.

1.3 Step 2: Demonstrate JULES performance with Mead runs forced with observed climate, LAI, height

Plots of modelled GPP (blue) against observed GPP (green) are shown in Figure S2-1 for years in which soybean is grown in the Mead FLUXNET irrigated site US-Ne2. The general model seasonality and magnitude of GPP match the observations for all years, in 2006 and 2008 there is a slight overestimation of GPP in early summer. The overestimation of GPP during the senescence period (particularly 2004 and 2008) could be explained by the model limitation that the model Vcmax(25)stays constant whereas in reality it would decline over the growing season. Including this decline in JULES would result in a closer fit between the observed and model GPP.

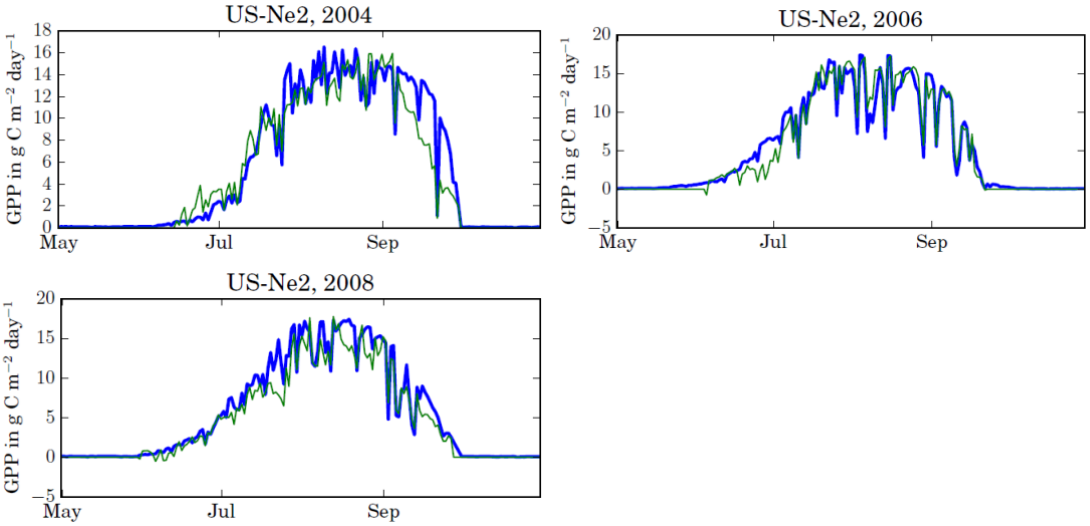

Figure S2-1 Time series of Gross Primary Productivity for irrigated soybean at the Mead FLUXNET site US-Ne2. Blue: JULES model without the crop model; LAI and canopy height prescribed and the 'new' input parameters in Table 3, Table 2.

1.4 Step 3 Tune parameters needed by JULES-Crop CFTs

1.4.1 Carbon partitioning

The carbon partitioning parameters a, b were tuned to observations of the biomass of green leaves, yellow leaves, stem and reproductive parts of soybean. The ratio of carbon to biomass in each part of the plant was assumed to be constant in time.The C_{leaf} pool in the model contains green leaves only because it directly link to photosynthesis and LAI. The C_{harv} pool consists of both the yellow leaves and reproductive parts of the plants. Stem carbon in the model is split between the C_{resv} and C_{stem} pools. The Mead biomass observations were linearly interpolated to a daily time series and differentiated to the respective development index (DVI).

According to Figure S3-1, the tuned parameters (dashed lines) show an improvement of the amount of carbon to

the observation compared to the Osborne et al., (2015) parameters. For green leaves and harvest carbon pool, Osborne et al., (2015) overestimate the amount of carbon while the stem carbon is underestimated. The tuned parameters fixed this and fit the observation.

Figure S3-1 shows the tuned partition fractions more clearly together with the tuned functions given by de Vries et al. (1989). $\beta root$ was calculated by using the constraints from leaf, stem and harvest carbon as root carbon observation is not available for the Mead site.

1.4.2 Crop height

Maximum crop height and stem biomass measurements in each year from the Mead FLUXNET sites were used to tune for the allometric constants λ, κ shown in Figure S3-2. The tuned parameters (dashed line) fit better than the Osborne et al. (2015) parameters (solid line) especially when the dry stem biomass is larger than 0.25 kg m^{-2}.

1.4.3 Specific Leaf Area

The parameters governing the relation between DVI and Specific Leaf Area (SLA) (γ and δ) are tuned in Figure S3-3. Note that the original and the tuned relations have a very different behaviour at low DVI. This could be an issue, as the model is very sensitive to SLA at the beginning of the crop season and this is not well constrained by the observations. Observations showed that soybean in the early growing stage have thin leaves but larger leaf area to intercept more light when space is less constrained. At a later growing stage when the soybean canopy become dense it tends to grow thicker leaves to intercept more sunlight, hence the higher SLA at DVI after 1.

1.4.4 Carbon to biomass ratio in stem and leaves

The carbon to biomass fractions in the leaf, stem, root, and harvest pools are set to 0.46, 0.49, 0.47, 0.53 respectively, from de Vries et al., (1989). The carbon to biomass ratio in the leaves used in Osborne et al., (2015) and the value used here are both plotted in Figure S3-4.

1.4.5 Initial amount of carbon in crops

In JULES-crop we assumed that approximately half of the plant carbon C_{init} is above ground near emergence DVI = 0.1. The initial value of carbon is very sensitive to the thermal time for emergence. Figure 7 shows that the C_{init} at DVI=0 is too high to be consistent with the above-ground biomass observations, we tuned it to the lowest value from observation (Figure S3-5).

1.4.6 Respiration

New respiration parameters can be derived from the tables in de Vries et al., (1989), using the method described in Williams et al., (2017). This leads to different r_g for each carbon pool: 0.32, 0.39, 0.23 and 0.24 for leaf, harvest, stem and root pools respectively, which cannot be accounted for in JULES. We use the r_g in this configuration for leaves but note this source of error. Using de Vries et al., (1989) gives μ_{sl}=0.51 (using τ =0.26), μ_{rl}=0.39. Using de Vries et al., (1989) also gives f_d=0.0038/0.85 to 0.0056/0.85 i.e. 0.0045 to 0.0067 (the factor 0.85 is from assuming 50% of leaves during day have light inhibited respiration). In order to fit this parameters, we perform JULES-crop runs at the irrigated site US-Ne2 (with the parameters from Table 3, Table 2 and model flags in Table 1), and tune the parameters to match the aboveground carbon at harvest (Figure S3-1). This leads to a value of f_d=0.008 (note this is much less than the default JULES value of 0.015). These respiration

parameters are poorly constrained in this configuration and are therefore a significant source of error. However, with these settings, the modelled GPP, LAI, crop height and carbon in the harvest pool are good matches to the observations.

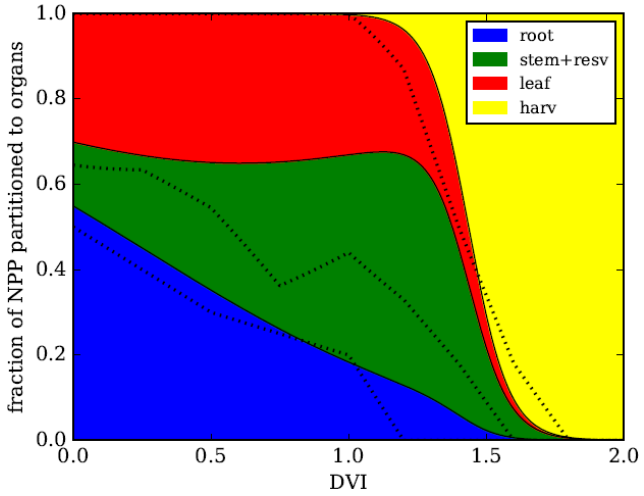

Figure S3-1. Partition fractions as a function of Development Index (DVI) using the tuned parameters. The dotted lines are from de Vries et al. (1989). (DVI;0 = emergence, 1=flowering, 2 = maturity).

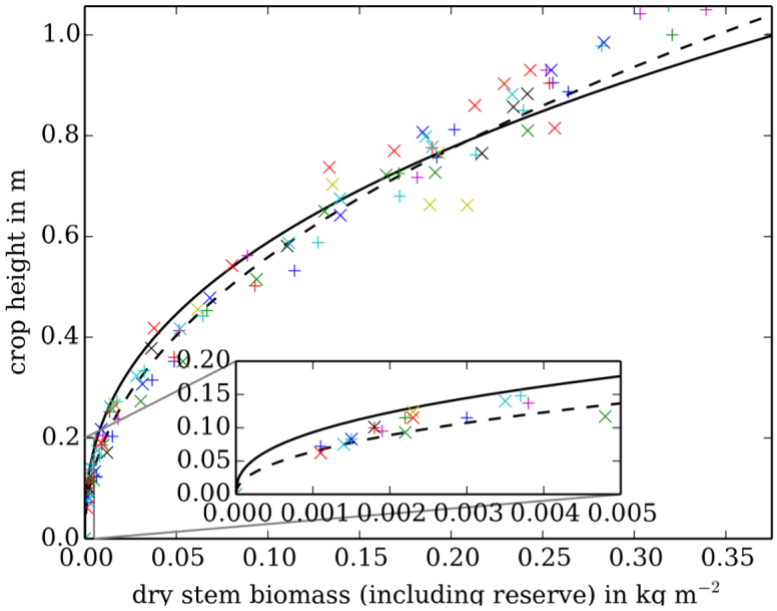

Figure S3-2. Crop height against dry stem biomass (including reserves). Vertical crosses (+) and diagonal crosses (x) are US-Ne2 and US-Ne3 observations respectively. Solid line shows the fit using parameters from Osborne et al., (2015) and dashed line shows a tuned fit. Only points up until the maximum stem biomass for that site in that year are plotted.

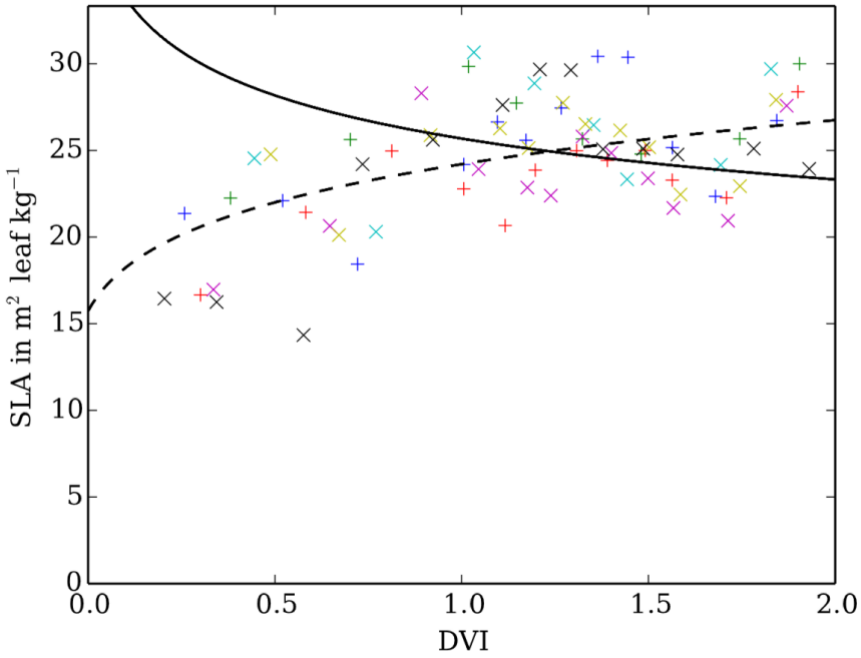

Figure S3-3. Specific leaf area against DVI. Vertical crosses (+) and diagonal crosses (x) are US-Ne2 and US-Ne3 observations respectively. Solid line shows the fit using parameters from Osborne et al., (2015) and dashed line shows a tuned fit.

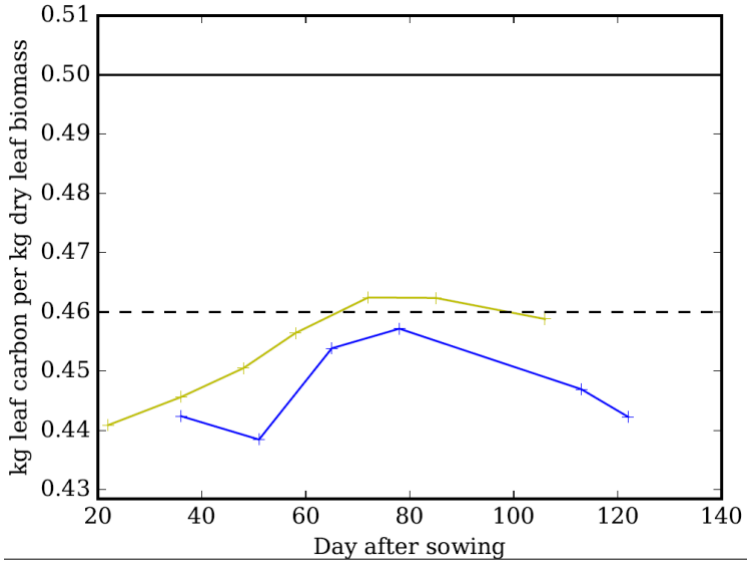

Figure S3-4. Carbon to biomass ratio in leaves against day after sowing at US-Ne2 (blue: 2002, yellow: 2004). Solid black line shows the value used in Osborne et al., (2015), dashed black line shows the value used in this analysis.

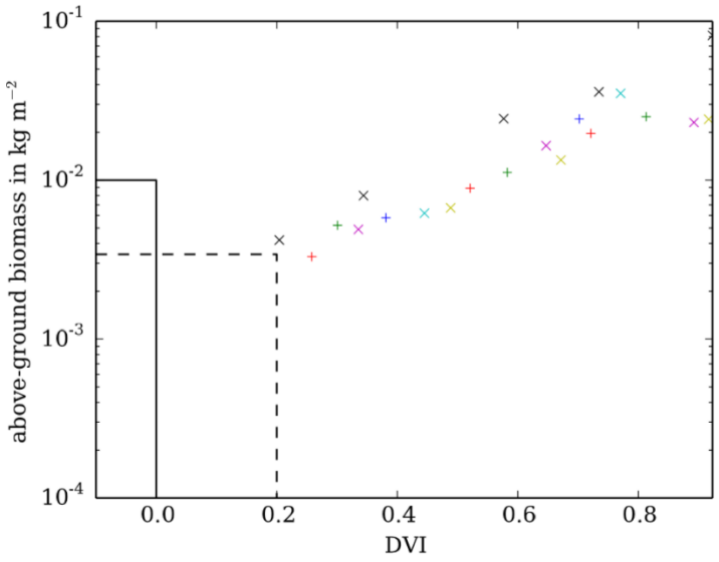

Figure S3-5. Above-ground biomass measurements against DVI. Vertical crosses (+) and diagonal crosses (x) are US-Ne2 and US-Ne3 observations respectively. Intersection of the solid black line shows the initialisation used in Osborne et al., (2015), intersection of dashed black line shows the initialisation used in this study.

190

1.5 Step 4 and 5: Demonstrate JULES-Crop performance with Mead runs forced with derived NPP

This section describes the results from the runs for the Mead site with the parameter settings summarised in Tables 2 and 3 and crop model switched on. We then carried a standard JULES-crop run with the new tuning and compared the results of green leaf, harvest, stem and reserve biomass with Osborne et al., (2015) (Figure S4-1).
195 We then further validated the new tuning performance using LAI, canopy height, above ground biomass and harvest carbon observation (Figure S4-2). The reduction in modelled LAI compared to observations was deliberately introduced when tuning the senescence parameters. In Figure S4-2, the modelled LAI is slightly underestimate during the peak LAI around September, but it generally reproduces the seasonality of the observation. The observed canopy height has a maximum height that coincide with the maximum LAI, the
200 observed canopy height shows a slight decrease after the peak, but the model shows a flat plateau until the crop is harvested. The above ground biomass also shows a similar pattern as the canopy height. For carbon in the harvest pool, the model shows a slight underestimation of the maximum carbon in 2006 and 2008 compared to the observation but in general it shows a consistent value and seasonality. In Figure S4-3, the GPP simulated by JULES-crop with soybean parameters shows a very close agreement in terms of the seasonality and the value of
205 GPP.

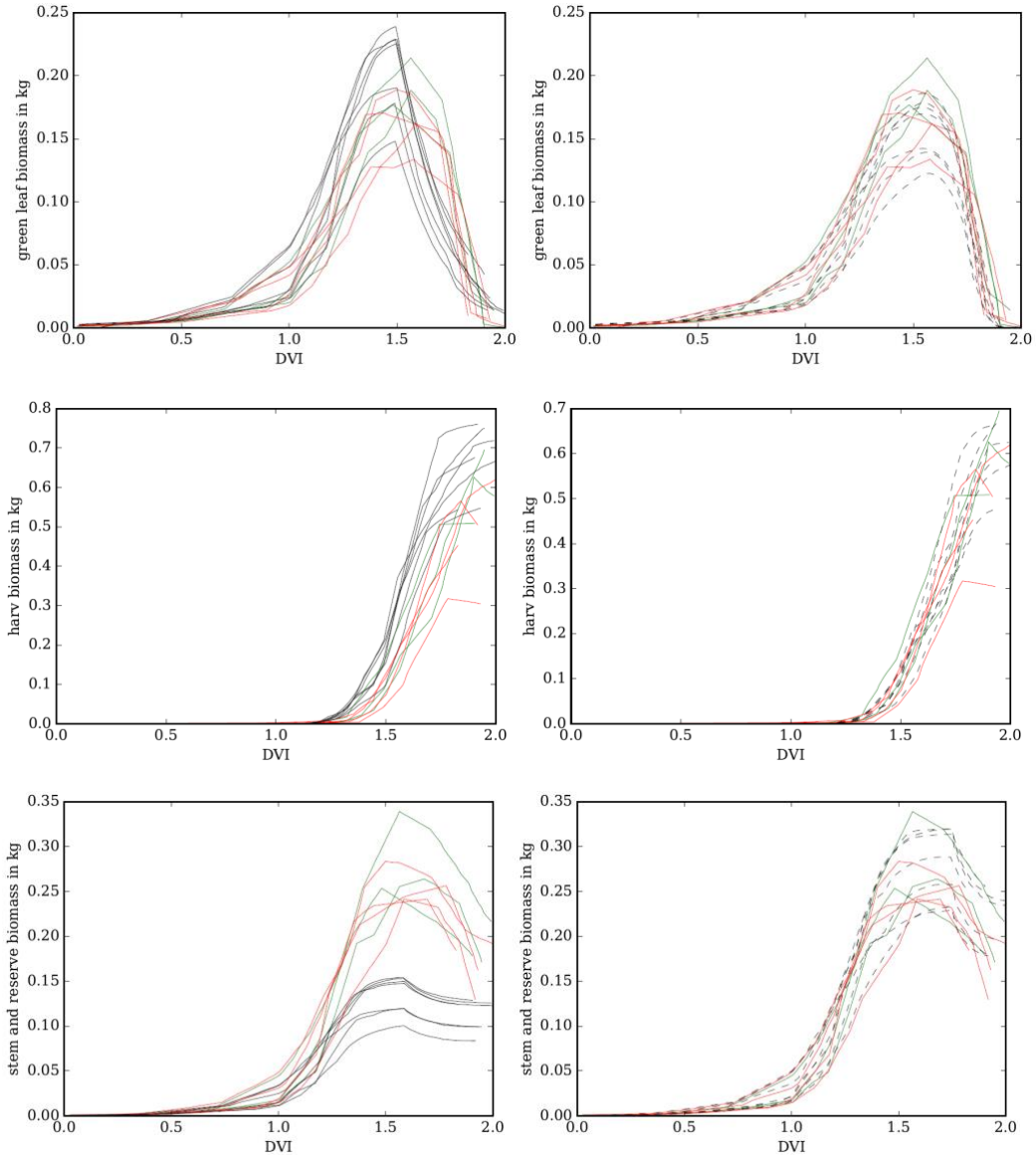

Figure S4-1. These plots use the observed change in aboveground carbon together with the partition fractions, senescence parameters and remobilisation parameters in JULES-crop to estimate leaf carbon (top), harvest carbon (middle) and stem carbon (bottom) in JULES respectively (black lines). The green and red lines are observed leaf carbon, harvest carbon and stem carbon. Green is site US-Ne2 (irrigated) and red is site US-Ne3 (rainfed). The left panel uses the Osborne et al., (2015) parameters (black solid line) and the right panel uses the new, tuned parameters (black dashed line). (DVI:0 = emergence, 1=flowering, 2 = maturity).

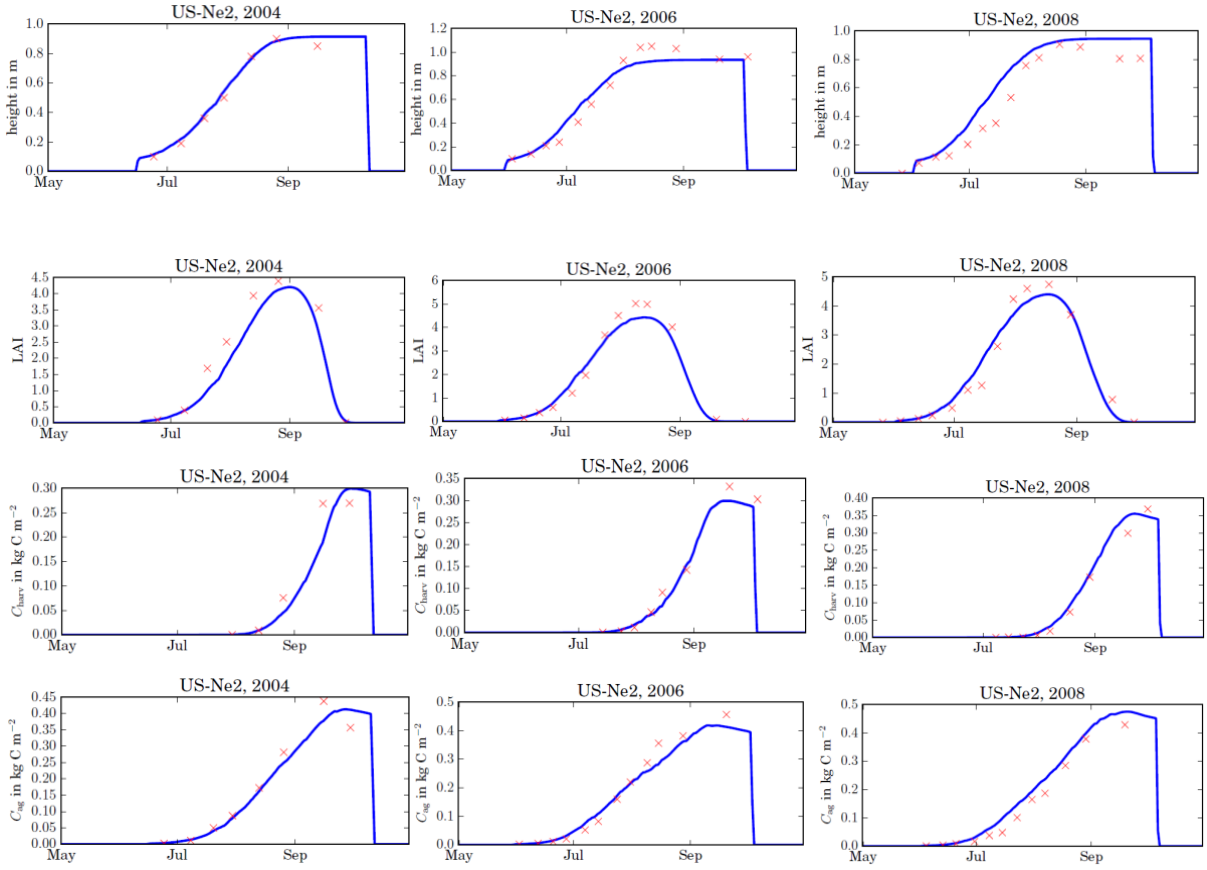

Figure S4-2. Time series from top to bottom: Leaf Area Index, canopy height, above ground biomass and carbon in the harvest pool (reproductive part of the crop and yellow leaves) for irrigated soybean at the Mead FLUXNET site US-Ne2. Blue: model, red: observations from Mead FLUXNET site US-Ne2. JULES runs have the crop model switched on and the input parameters in Table 3, Table 2.

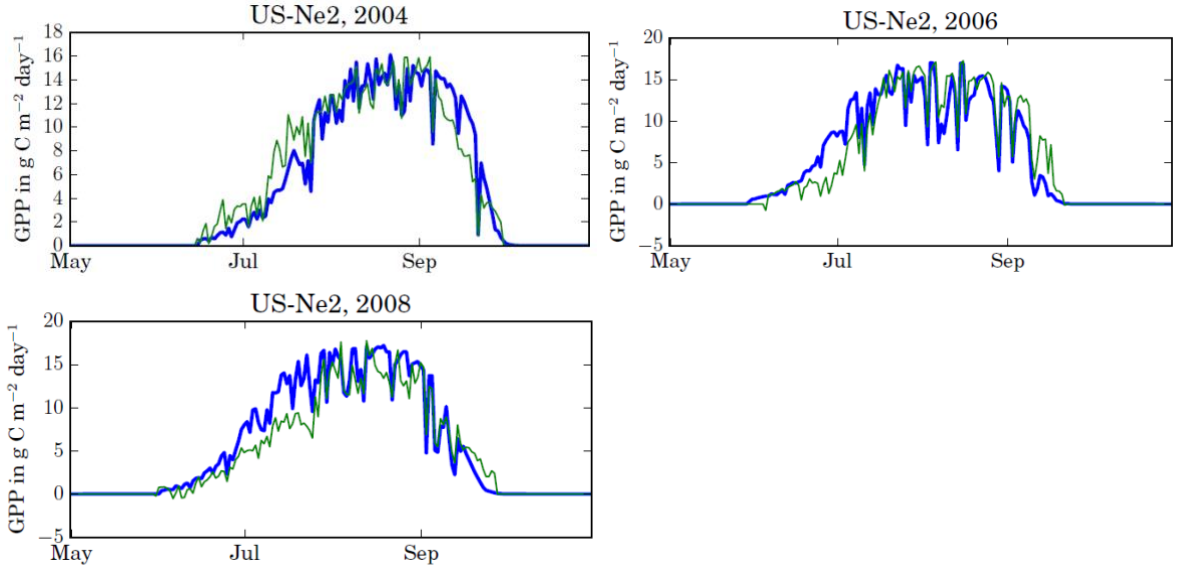

Figure S4-3. Time series of Gross Primary Productivity for irrigated soybean at the Mead FLUXNET site US-Ne2. Blue: JULES model with soybean parameters and crop model turned on; green: observations. Simulated

results are from JULES-crop with input parameters specified in Table 2,3,4; observations are from the Mead FLUXNET site US-Ne2.

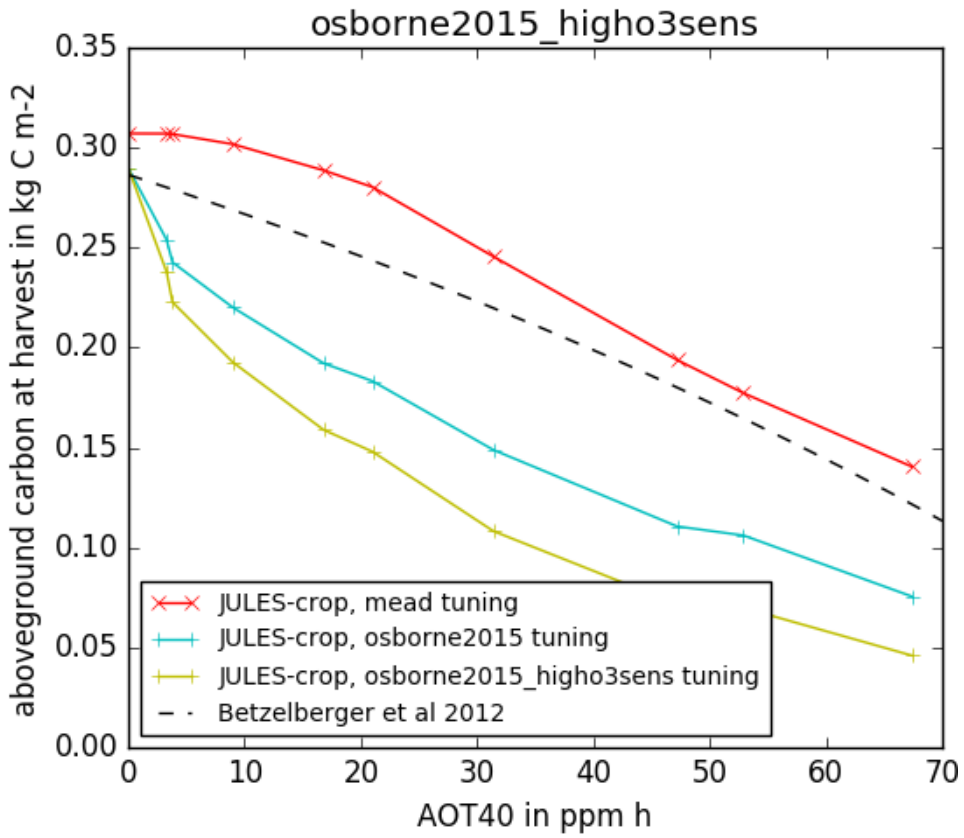

Figure S5-1. Aboveground carbon at harvest stage for different tunings at various ozone concentration when JULES parameter p0=0 (water stress)

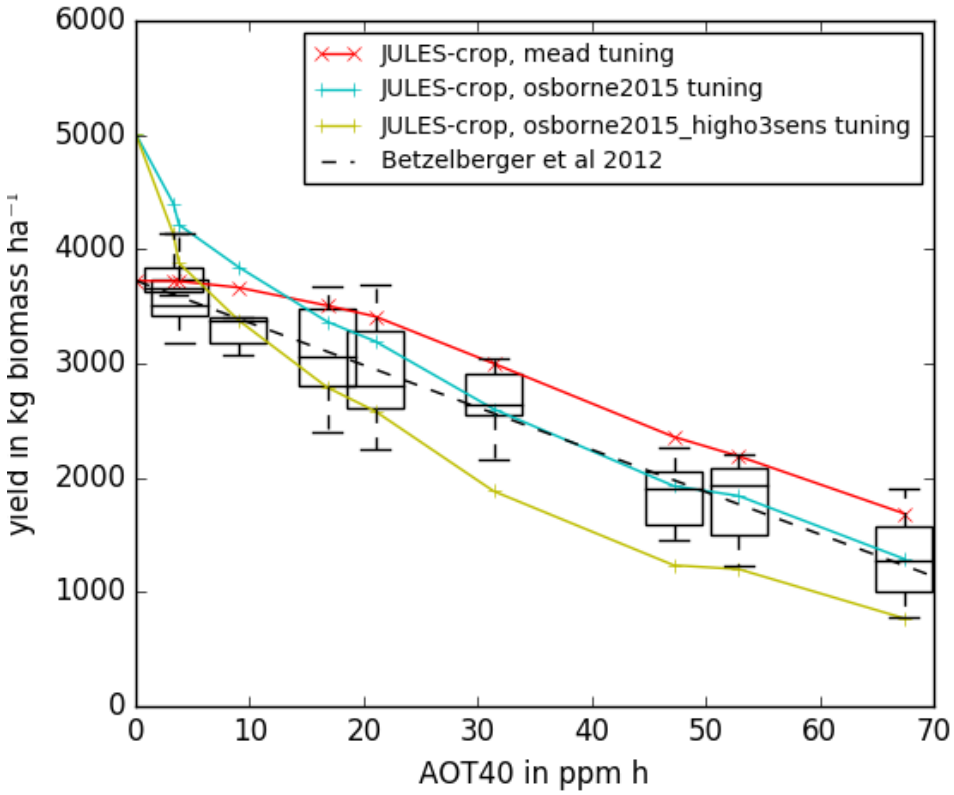

Figure S5-2. Modelled and observed yield at different ozone concentration when JULES parameter p0=0 (water stress)

280 Table S1 Summary of Land Surface Models (LSM) that contains crop tiles

Crop model	Land Surface Model	Crops Function Type	Scale	Ozone damage on vegetation
LPJ-ml (managed land)	LPJ-GUESS (Bondeau et al., 2007)	13 types of 11 arable crops and 2 managed grass types	Global	No
CLM-CROP	CESM (Community Land Model for Community Earth System Model) (Levis et al., 2011)	Four major crops: maize, soybean, rice and wheat	Global	Yes (Zhang et al., 2018)
Agro-IBIS	IBIS (Kucharik et al., 2003)	12 natural and five crops: Maize, soybean, wheat, *Miscanthus giganteus*, sugarcane	Continental US	In development
ORCHIDEE-CROP	ORCHIDEE (Gervois et al., 2004; Berg et al., 2010, Wu et al., 2016)	Ten natural and Wheat, maize, soybean, sugarcane and more varieties	Europe and other regions	In development
JULES-Crop	JULES (Clark et al., 2011; Osborne et al., 2015)	4 Crop Functional types, divided into C3 and C4. Potentially 12 crop functional types	Global	Yes. Flux-gradient approach to quantify O_3 interactive effects.
SIB	Simple Biosphere model (Lokupitiya et al., 2009)	Maize, soybean, wheat	North America	No
ISAM	Integrated Science Assessment Model (Song et al., 2013)	Maize-soybean rotation	North America	No

285

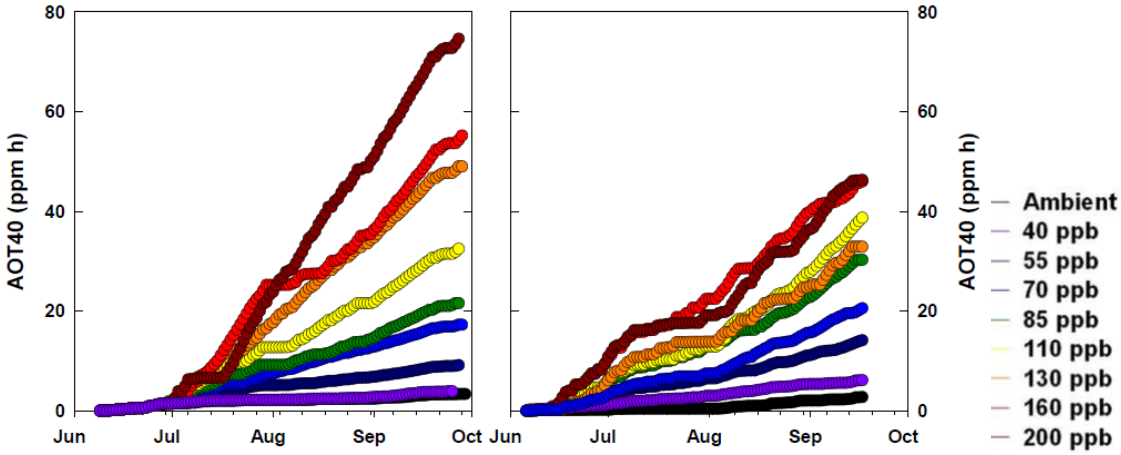

Figure S6 AOT40 measured at SoyFACE in 2009 (left) and 2010 (right). With different target concentration. (Betzelberger et al., 2012)